

# Dual-Material Minimum Weight Structures Fabrication Using Ultrasonic Consolidation

Obielodan J.O<sup>1</sup> and Stucker B.E<sup>2\*</sup>

<sup>1</sup>Mechanical and Aerospace Engineering Department, Utah State University, Logan, UT 84322

<sup>2</sup>Industrial Engineering Department, University of Louisville, Louisville, KY 40292

Reviewed, accepted September 23, 2010

## Abstract

The multi-material capability of additive manufacturing (AM) processes has created opportunities for structural designs that would otherwise be impossible. This work involves the development of a methodology for fabricating dual-material minimum-weight structures using ultrasonic consolidation (UC). Sample structures were designed, fabricated and tested for load carrying capabilities. Analyses of results show that dual-material minimum weight structures made of Al3003/MetPreg<sup>®</sup> and Al3003/Ti composite material members can withstand significantly higher strain energy densities up to the point of failure than similar structures made of Al 3003 alone. This is an indication that UC can be effectively used to fabricate multi-material structures for real life applications.

## 1 Introduction

Research on the fabrication of multi-material structures using different additive manufacturing (AM) processes has accelerated in recent years. AM processes have the potential for flexible variation of materials and microstructures, both in continuous and discrete fashion in addition to their capabilities for complex geometry structures. New uses of some advanced materials are being discovered because of the ability to combine them with other materials in AM fabricated structures. Also, some of the materials that would otherwise be difficult to combine in conventional processes are being processed (Cohen et al., 2006; Malone et al., 2004; Liu and DuPont 2003; Griffith et al., 1997; Arcaute et al., 2009; Janaki Ram et al., 2007; Obielodan et al., 2010B). This ability to deposit function specific materials where they are needed in a structure further revolutionizes engineering structure design and material usage. One of the driving forces is the economic use of costly advanced materials that are prescribed to be deposited just where they are functionally required in a structure. The application of these capabilities is diverse, ranging from medical to aerospace, automobile, nuclear and others.

Potential applications of multi-material structures fabricated using AM processes have been demonstrated. Arcaute *et al.*, 2009, used stereolithography (SL) for the fabrication of multi-material scaffolds with spatially controlled characteristics for tissue engineering applications. Also, Wicker *et al.*, 2004, fabricated complex multi-material hydrogel constructs for nerve regeneration and guided angiogenesis applications. Meso and macro scale multi-material structures have also been fabricated using SL (Jae-Won Choi *et al.* 2009 and Inamdar *et al.* 2006).

Objet Geometries Limited commercialized the 3D printing of dissimilar material end use products using polymer materials ([www.growit3d.com/services/multi-material-polyjet](http://www.growit3d.com/services/multi-material-polyjet)). Objet's Connex™ machines jet multiple materials simultaneously to fabricate multi-material structures.

Different laser powder metal deposition processes have been used to deposit multi-material structures. Examples include gradient structures (Griffith et al., 1997, Liu and DuPont, 2003), surface cladding with corrosion and wear resistant materials for machinery (Foroozmehr et al., 2009) and medical implants applications (Janaki Ram and Stucker, 2008). Both 3D printing and laser powder deposition processes have capabilities for continuous material variation as well as discrete material domains in fabricated multi-material structures.

Ultrasonic consolidation has been demonstrated to have the capabilities for multi-material structures fabrication. This capability was demonstrated by Janaki Ram *et al.*, 2007B, in their work in which copper, brass, nickel, inconel 600, AISI 347 stainless steel, stainless steel AISI 304 wire mesh, MetPreg®, and aluminum alloy 2024 were each welded to aluminum alloy 3003-H18. Domack and Baughman, 2005, investigated the capability of UC to fabricate graded titanium and nickel alloy multi-material structures. Additionally, ultrasonic welding has been successfully used to weld metals to a polymer matrix composite (Kruger *et al.*, 2004). Obielodan *et al.*, 2010B, further demonstrated UC multi-material capabilities by welding different combinations of molybdenum, tantalum, titanium, copper, silver, nickel, MetPreg®, aluminum alloys 1100, 3003, 6061 and boron powder. Also, the shear strengths of titanium/aluminum ultrasonically bonded foils were characterized by Obielodan et al., 2009.

Ultrasonic consolidation, described more fully elsewhere (White, 2003 and Obielodan *et al.*, 2010A), is a low temperature process that combines ultrasonic welding and additive manufacturing technology. Multi-material structures fabricated using UC characteristically have

discrete material domains as opposed to the continuous material variation that is obtainable with laser powder deposition processes and 3D printing. The process has the potential for fabricating structures for applications in systems subjected to mechanical loading. In this study, a methodology for fabricating multi-material structures using UC was developed. UC structures with a single material are relatively easy to fabricate when compared to multi-material fabrications, as foils can be automatically fed.

Multi-material minimum weight Michell structures (Dewhurst, 2001; Dewhurst, 2005; Selyugin, 2004 and Michell, 1904) represent one of the categories of structures that can be geometrically and materially complex to fabricate using conventional processes. They are made of multiple, thin members that are preferably made from light weight materials with high specific strength and stiffness. Such structures are readily applicable to aerospace and automotive industries, where there is continuous emphasis on higher strength and lower weight structures for improved fuel efficiency and performance. Figure 1 shows an example of a complex minimum weight structure with members that could be made of different materials based upon Michell theory (Michell, 1904). In the illustrated structure, if the structure is pinned at points A and B and a load is placed at C, parallel to a line between A&B, as shown with the arrow, the outer member labeled D will be in pure compression, as well as all the inner members that join D tangentially. Those inner network members that are perpendicular to D, and the member between A and C will be in pure tension. In order to optimize a structure to its fullest extent, the members in tension can be made of materials different from those in compression. In this case, the intersection between the tensile and compressive members and the design and strength of these joints is of critical importance for the structure's reliability and performance.

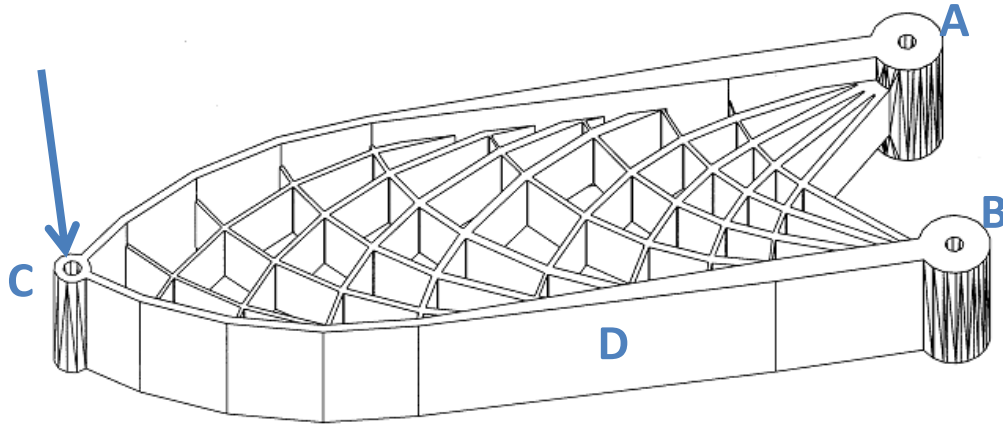


**Figure 1: A minimum weight structure design (Dewhurst, 2001)**

Simplified minimum weight structures based on maximum strength and maximum stiffness criteria (Dewhurst, 2005) were designed and fabricated. Figure 2 shows a free body diagram of the structure with  $oa$ ,  $ob$  and  $oc$  as compression members and  $ab$  and  $ac$  as tension members when subjected to compressive load  $F$  with simple supports at  $b$  and  $c$ . Given a simplified minimum weight structure shown in Fig. 2 with

$$\text{span} = L,$$

$$\text{applied force} = F,$$

$$F = f\sqrt{2},$$

where,  $f$  is the stress acting on the tension members at any point during loading. Table 1 shows the load relationships existing in the structure members. Structures designed based on maximum stiffness criterion must satisfy the following strain ratio (Dewhurst, 2005)

$$\frac{\varepsilon_T}{\varepsilon_C} = \left[ \frac{\left( \frac{\rho_T}{E_T} \right)}{\left( \frac{\rho_C}{E_C} \right)} \right]^{\frac{1}{2}} = \left( \frac{E_C \rho_T}{E_T \rho_C} \right)^{\frac{1}{2}} \quad (i)$$

In this work, simple dual-material minimum weight structures consisting of MetPreg<sup>®</sup>/aluminum alloy 3003 composite as tension members and aluminum alloy 3003 as compression members were fabricated. Samples with titanium/aluminum alloy 3003 and aluminum alloy 3003 as separate structural members were also fabricated. Both maximum strength and maximum stiffness design criteria were used for the design of the fabricated structures

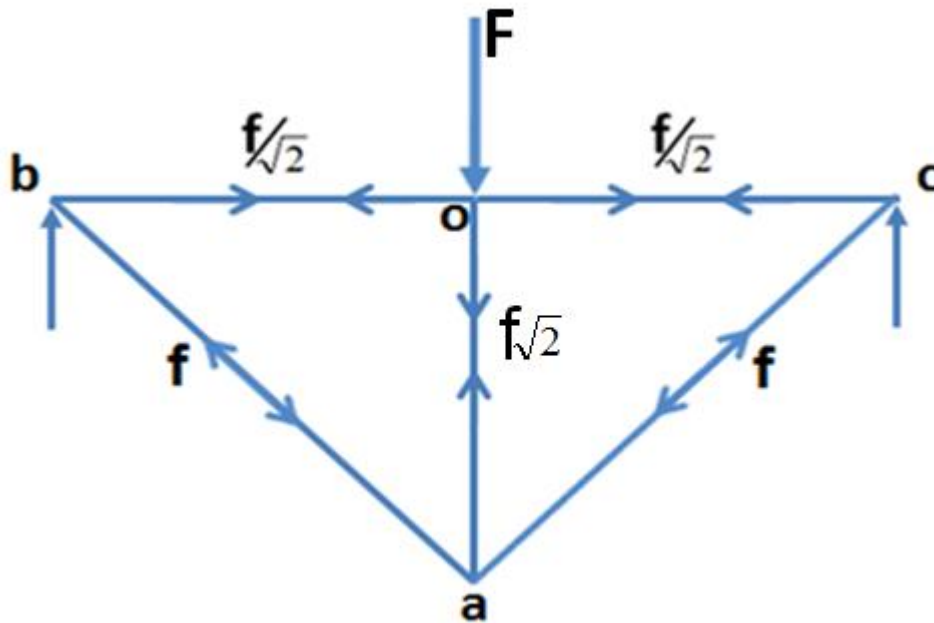


**Figure 2: Free body diagram of the dual-material minimum weight structure**

**Table 1: Load and Size Relationship for Minimum Weight Structure**

Element	Length	Force	Cross-sectional area
<i>oc</i>	$L/2$	$F/2 = f/\sqrt{2}$	$F/(2\sigma_c)$
<i>oa</i>	$L/2$	$F = f\sqrt{2}$	$F/(\sigma_c)$
<i>ac</i>	$L/\sqrt{2}$	$F/\sqrt{2} = f$	$F/(\sqrt{2}\sigma_T)$

## 2 Experimental Work

A Solidica Formation™ ultrasonic consolidation machine was used for all the fabrications in this work. During typical operation, the machine uses an automatic foil feeding mechanism, but foil materials can be fed manually when it is necessary. The parts were made on aluminum alloy 3003-H18 substrate materials of 355 x 355 x 12 mm size, mounted on a heat plate. Foil materials of aluminum alloy 3003-H18, MetPreg® and CP titanium were used for the fabricated structures. The structures are composed of tension and compression members. The tension members carry simple tensile loads while the compression members carry simple compressive loads when a three-point load is applied as illustrated in Fig. 2. One set of the structures consist of MetPreg®/Al3003 composite tension members and Al3003 compression members. The other set was made of titanium/Al3003 composite tension members and Al3003 compression members. Both maximum stiffness and maximum strength minimum weight structure design criteria were used for each material combination. Thus, for MetPreg®/Al3003 composite and Al3003 material combination, the two criteria were used to design structures having different member sizes. The same criteria were applied for the titanium/Al3003 and Al3003 material combination. Three structures were fabricated using each criteria and material combination.

A third set of structures were ultrasonically consolidated exclusively with Al 3003-H18 foil material using the dimensions of the MetPreg®/Al 3003 material minimum weight structures. Another set of structures were fabricated using wrought Al 3003 H-18, having the same base material as the Al 3003 foil used. These last sets of structures were fabricated as single material copies of the shape and sizes of the MetPreg® and titanium reinforced dual-material structures

described above. All the single material structures were fabricated for the sole purpose of comparing their load carrying capabilities with those of the dual-material structures. The major comparison factor is the strain energy densities of the structures at failure.

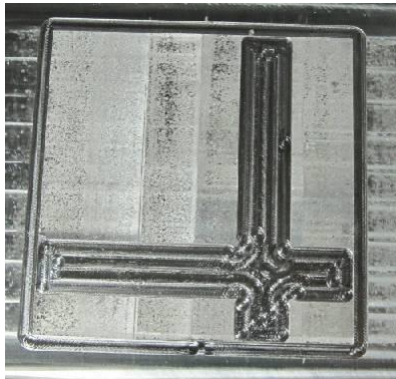
For the purpose of analysis and discussion in this work, the structures have been named as follows. All structures designed based upon maximum strength design criterion or single material copies of such designs have their labels hyphenated with “STR”. Similarly, those designed based upon maximum stiffness criterion or their single material copies have their labels hyphenated with “STF”. Thus, MetPreg<sup>®</sup>/Al 3003 dual-material structures designed based on maximum strength criterion are labeled Met-STR, while structures of the same materials designed based on maximum stiffness criterion are labeled Met-STF. Corresponding structures designed based on Ti/Al 3003 materials are labeled Ti-STR and Ti-STF. The single material direct copies of Met-STR and Met-STF structures ultrasonically consolidated using Al 3003 foils are correspondingly labeled Al-STR and Al-STF. Also, those machined out directly from Al 3003-H18 plate as single material structure copies of Met-STR and Met-STF are correspondingly labeled W-Al-MSTR and W-Al-MSTF, while copies of Ti-STR and Ti-STF are respectively labeled W-Al-TSTR and W-Al-TSTF. The sizes of the members of the fabricated structures are shown in Table 2.



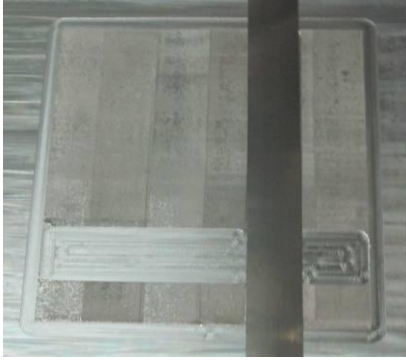
**Table 2: Member Sizes for Fabricated Structures**

Structure	Sample	Member widths (mm)			Thickness (mm)
		<i>oa</i>	<i>oc</i>	<i>ac</i>	
Met-STR	1	12.00	6.00	3.05	3.85
	2	12.00	6.00	3.05	3.57
	3	12.00	6.00	3.05	3.00
Met-STF	1	10.00	5.00	4.91	3.22
	2	10.00	5.00	4.91	3.63
	3	10.00	5.00	4.91	3.45
Ti-STR	1	8.00	4.00	6.00	3.00
	2	8.00	4.00	6.00	3.15
	3	8.00	4.00	6.00	3.00
Ti-STF	1	8.00	4.00	5.16	2.87
	2	8.00	4.00	5.16	3.57
	3	8.00	4.00	5.16	3.23
Al-STR	1	12.00	6.00	3.05	4.10
	2	12.00	6.00	3.05	4.13
	3	12.00	6.00	3.05	3.70
Al-STF	1	10.00	5.00	4.91	4.00
	2	10.00	5.00	4.91	3.86
	3	10.00	5.00	4.91	3.89
W-Al-MSTR	1	12.00	6.00	3.05	3.30
	2	12.00	6.00	3.05	3.30
	3	12.00	6.00	3.05	3.18
W-Al-MSTF	1	10.00	5.00	4.91	3.14
	2	10.00	5.00	4.91	3.30
	3	10.00	5.00	4.91	3.46
W-Al-TSTR	1	8.00	4.00	6.00	3.46
	2	8.00	4.00	6.00	3.24
	3	8.00	4.00	6.00	3.03
W-Al-TSTF	1	8.00	4.00	5.16	3.34
	2	8.00	4.00	5.16	3.05
	3	8.00	4.00	5.16	3.00

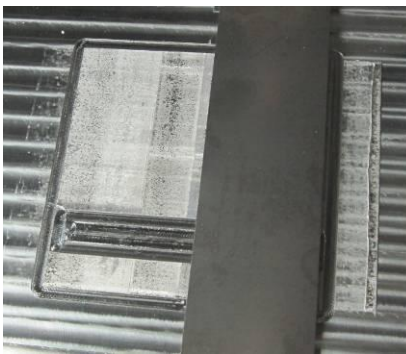
Four different machine codes were developed using Initial Graphics Exchange Specification (IGES) 3-D model files for each of the dual material structures. This became necessary as the UC machine needed to operate in an unconventional sequence characterized by interruptions while changing from one file to the other because of the different materials used. The first code was for consolidating the Al 3003 matrix material of 100 x 105 x 0.3mm consisting of two layers of foils. After the consolidation, the integrated 3-axis CNC milling facility was used to machine out the channels for accommodating the embedded reinforcing materials. This was used to accommodate the reinforcing materials for the respective tension members in the fabricated structures. The MetPreg<sup>®</sup> foil was embedded in 9.5mm wide cavities while that for the titanium foils was 12 mm. This first step is illustrated in Fig.3a.



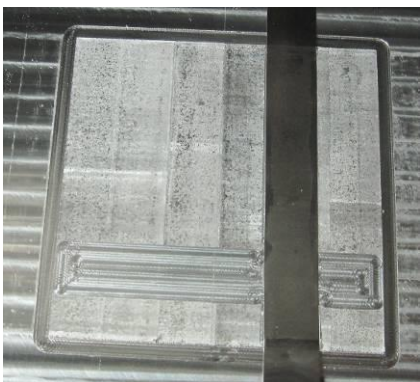
**(a): Cavity machined into deposited Al 3003 matrix**



**(b): Reinforcing foil placed in position**



**(c): Titanium foil of equal width with the sonotrode placed on top of reinforcing foil preparatory to indirect welding**



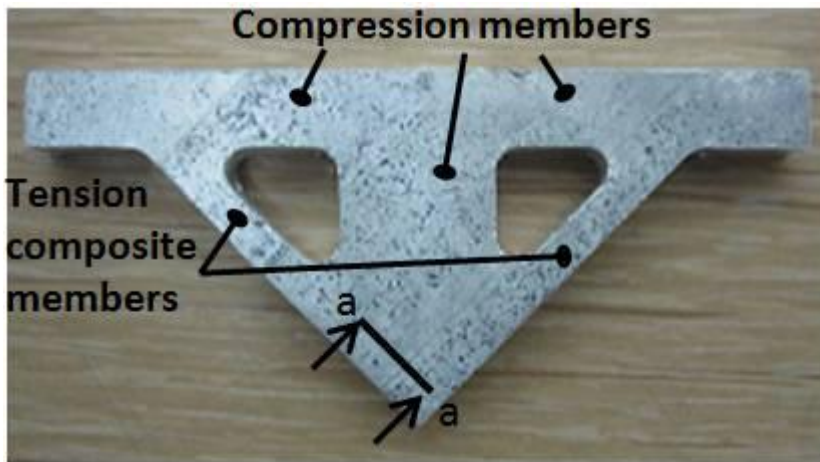
**(d): The first reinforcing foil fully welded into the Al 3003 matrix**



**(e): The second reinforcing foil fully welded into the Al 3003 matrix**



**(f): The structure profile machined using UC integrated CNC milling**



**(g): The structure removed from the substrate using conventional milling**

**Figure 3: Structure fabrication sequence**

The second and third machine codes were used to weld the reinforcing material that is sandwiched with Al 3003 foils in alternate layers to make the composite tension members in each of the structures. In the respective structures, the reinforcing materials serve to reinforce the Al 3003 matrix foils in the tension members. The composite reinforcing foils were put in place one at a time and welded indirectly by placing a 25mm width titanium foil between it and the welding sonotrode as shown in Figs. 3b to 3e. The indirect welding was to prevent the sonotrode from having direct contact with the softer Al 3003 matrix material because of the required high welding amplitude applied for the reinforcing materials. Direct welding can destroy the Al 3003 matrix material at the high welding amplitude. The structures' constituent materials were welded using different sonotrode vibration amplitudes as determined in earlier work by Obielodan *et al.*, 2010B. Table 3 shows the compositional, hardness and dimensional details of the materials used while Table 4 shows the welding parameters applied for their consolidation. The mechanical and physical properties of the materials are shown in Table 5.

**Table 3: Nominal Compositions, Crystal Structures and Hardness of Materials used (Obielodan et al., 2010B)**

<b>Material</b>	<b>Composition</b>	<b>Crystal Structure at UC Temperature</b>	<b>Micro- Hardness (Hv)</b>	<b>Thickness (<math>\mu\text{m}</math>)</b>
Al alloy 3003 H18	Al-1.2Mn-0.12Cu	FCC	80	150
Titanium	Ti-0.59Fe-0.38Mn	HCP	185	70
MetPreg <sup>®</sup>	Al <sub>2</sub> O <sub>3</sub> Short Fiber	-	600	200
Al matrix reinforced tape				

**Table 4: UC Process Parameter Values used for Each Material**

<b>Material</b>	<b>Amplitude (<math>\mu\text{m}</math>)</b>	<b>Speed (mm/s)</b>	<b>Normal Force (N)</b>	<b>Temperature (<math>^{\circ}\text{F}</math>)</b>
Al 3003	16	23.70	1750	300
Ti	28	10.58	2000	300
MetPreg <sup>®</sup>	28	12.70	1750	300

**Table 5: Some Mechanical/Physical Properties of the Materials**

<b>Material</b>	<b>Reinf. Material Vol. Fraction (%)</b>	<b>Stiffness (GPa)</b>	<b>Tensile strength (MPa)</b>	<b>Density (Kg/m<sup>3</sup>)</b>
MetPreg <sup>®</sup> /Al3003 Composite	66	129	500	3020
Ti/Al3003 Composite	25	77.1	232	2934
Al3003	-	68	200	2730

The cycle of operations described above were repeated until the desired final thickness of the structure was attained. Thereafter, the fourth machine code file was used to cut out the profile of the structure as shown in Fig. 3f in reverse order from top to the bottom using the integrated CNC milling head. The completed structure is shown in Fig. 3g. The fabricated structures were subjected to three-point loading using a short beam shear test fixture (ASTM D 2344) as illustrated in Fig. 4. A 50kN capacity Tinius Olsen tension testing machine was used to apply a compressive load at 0.5mm/min speed until the structure failed.

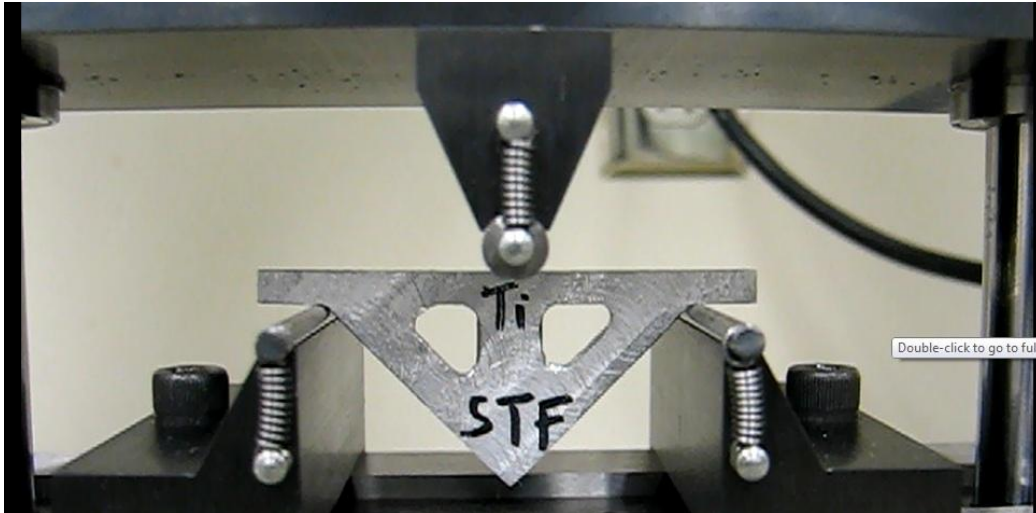


**Figure 4: Structure under test using a 3-point bend test fixture**

## **2.1 Metallographic Studies**

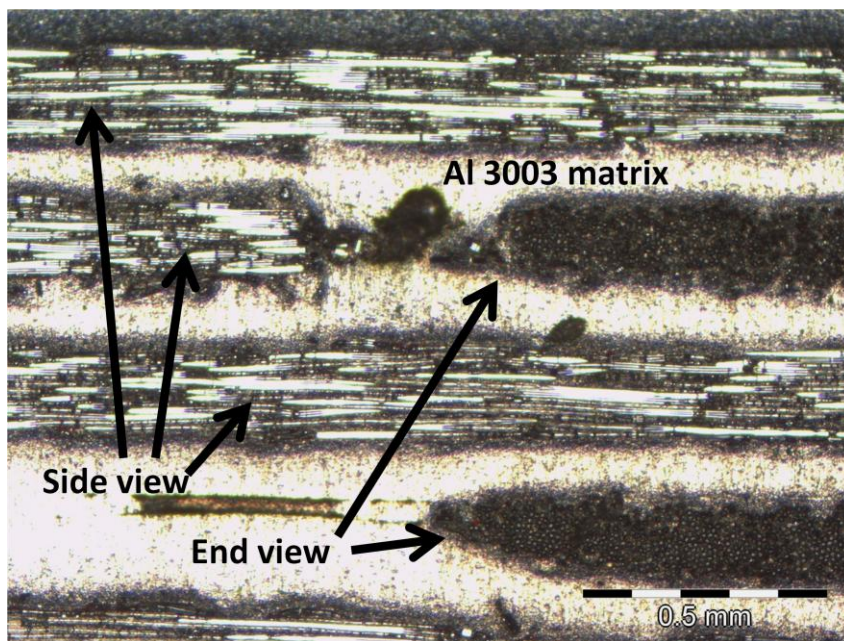
Small samples cut from the intersecting joints of the composite members as well as at their joints with the matrix material at the top of the structures were mounted and polished according to standard metallographic procedures. They were observed under optical microscope. Fractographic studies were also carried out on fractured surfaces of the structures.

## **3 Results and discussion**

### **3.1 Microstructures**

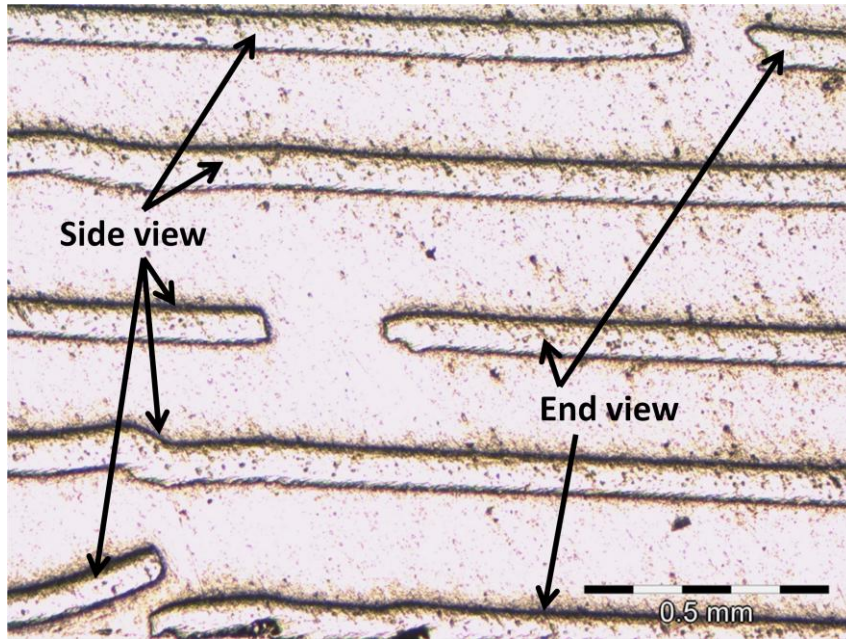
Micrographs of section a-a in Fig. 3g at the intersection joints of representative structures are shown in Fig. 5 below. Figure 5a shows the side and end views of reinforcing MetPreg<sup>®</sup> foils for the left and right hand side tension members respectively of the structure shown in Fig. 3g. MetPreg<sup>®</sup> foils for the left hand side tension member have their foils stretching through the length of the member in alternate layers. At the other layers, shorter reinforcing foils are seen with abutting joints with those of the right hand side tension member (that is, those with their end

views shown). Each of the reinforcing foil layers are alternated with the Al 3003 matrix material. The abutting reinforcing foil joints have gaps of varying sizes, because, they were manually laid without any tacking operation by the sonotrode. There is some measure of foil displacement of un-tacked foils during the welding operation resulting in the shift of positions. For structures reinforced with titanium foils, Fig. 5b shows corresponding foil arrangement at the intersection joint between the two tension members.



**(a): A view of interlocking MetPreg<sup>®</sup> foils in Al 3003 matrix at the intersection joints**





(a): A view of interlocking titanium foils in Al 3003 matrix at the intersection joints

**Figure 5: Micrographs of the interlocking foils at the intersection joints of reinforced structures. The side viewed and end viewed foils belong to the left and right tension members of Fig. 3g respectively**

### 3.2 Failure Strengths

Tables 6 and 7 shows the failure loads for each of the fabricated structures. It can be observed that the structures designed using maximum strength criterion failed at higher loads when compared to those fabricated using maximum stiffness criterion. The failure load data can however, not be used for direct comparison since the structures were not exactly of the same thickness. The more useful data based on calculated strain energy density at the point of failure is presented in Tables 8 and 9. They are also shown graphically in Fig. 6 and Fig. 7. The strain energy density values were calculated using

$$U = \frac{\sum(\frac{1}{2}\sigma\varepsilon v)}{V} \quad (ii)$$

Where,

$U$  = strain energy density for the structure

$\sigma$  = stress in each member at the point of failure

$\varepsilon$  = strain in each member at the point of failure

$v$  = volume of each member

$V$  = total structure volume

The stress  $\sigma$  in each member at the point of failure was calculated by normalizing the resolved load (based on Table 1 relationships) with respect to cross-sectional area. With the stress obtained, the strain  $\varepsilon$  was calculated using the stiffness value of each structure member.

The strain energy density data show that for structures of the same material combination, those designed based on maximum strength criterion generally have higher load carrying capacities than those designed based on maximum stiffness criterion. It is only in the case of Al-STR and Al-STF, ultrasonically consolidated using Al 3003 matrix material that structures based on maximum stiffness yielded higher average strain energy density.

**Table 6: Failure Load (N) Data for MetPreg<sup>®</sup>/Al 3003 Based Structures**

<b>Sample</b>	<b>1</b>	<b>2</b>	<b>3</b>
Met-STR	5190	4760	4140
Met-STF	4060	5020	4720
Ti-STR	3890	3760	4120
Ti-STF	3210	3360	3500
Al-STR	3120	3060	2530
Al-STF	4010	3840	3760

**Table 7: Failure Load (N) Data for Ti/Al 3003 Based Structures**

<b>Sample</b>	<b>1</b>	<b>2</b>	<b>3</b>
Ti-STR	3890	3760	4120
Ti-STF	3210	3360	3500
W-Al-STR	3200	3000	2730
W-Al-STR	2340	2230	2320

**Table 8: Strain Energy Density (N/mm<sup>2</sup>) Data for MetPreg<sup>®</sup> Based Structures**

<b>Sample</b>	<b>1</b>	<b>2</b>	<b>3</b>	<b>Average</b>
Met-STR	1.72E+05	1.67E+05	1.79E+05	172585.4
Met-STF	1.208E+5	1.45E+05	1.43E+05	136266.67
Al-STR	9.77E+04	8.02E+04	68289.06	82068.39
Al-STF	1.07E+05	8.64E+04	9.93E+04	97500
W-Al-STR	1.22E+5	1.11E+5	1.12E+5	115062
W-Al-STF	1.01E+5	9.69E+4	9.49E+4	97583

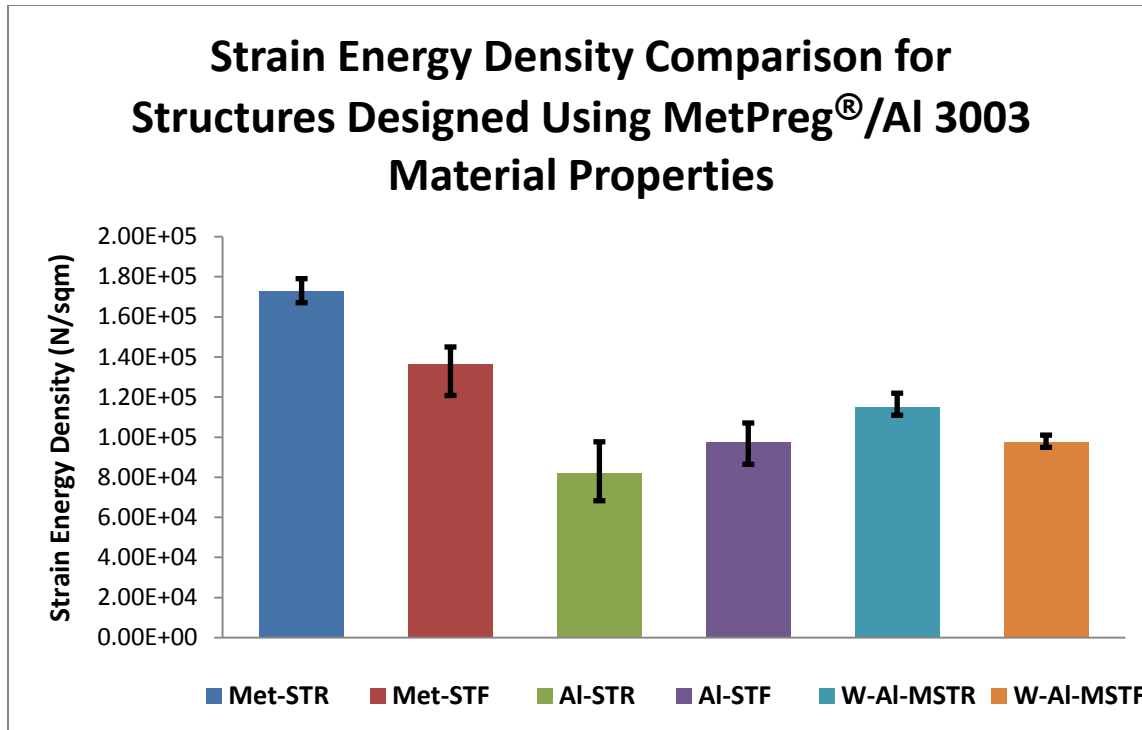


**Figure 6: Strain energy densities for structures designed based on MetPreg®/Al 3003 material properties**

**Table 9: Strain Energy Density (N/mm<sup>2</sup>) Data for Titanium Based Structures**

Sample	1	2	3	Average
Ti-STR	1.48E+05	1.38E+05	1.50E+05	1.45E+05
Ti-STF	1.48E+05	1.28E+05	1.13E+05	129621.8
W-Al-STR	8.16E+04	8.18E+04	7.75E+4	80288
W-Al-STF	6.27E+04	6.83E+04	7.64E+04	69132

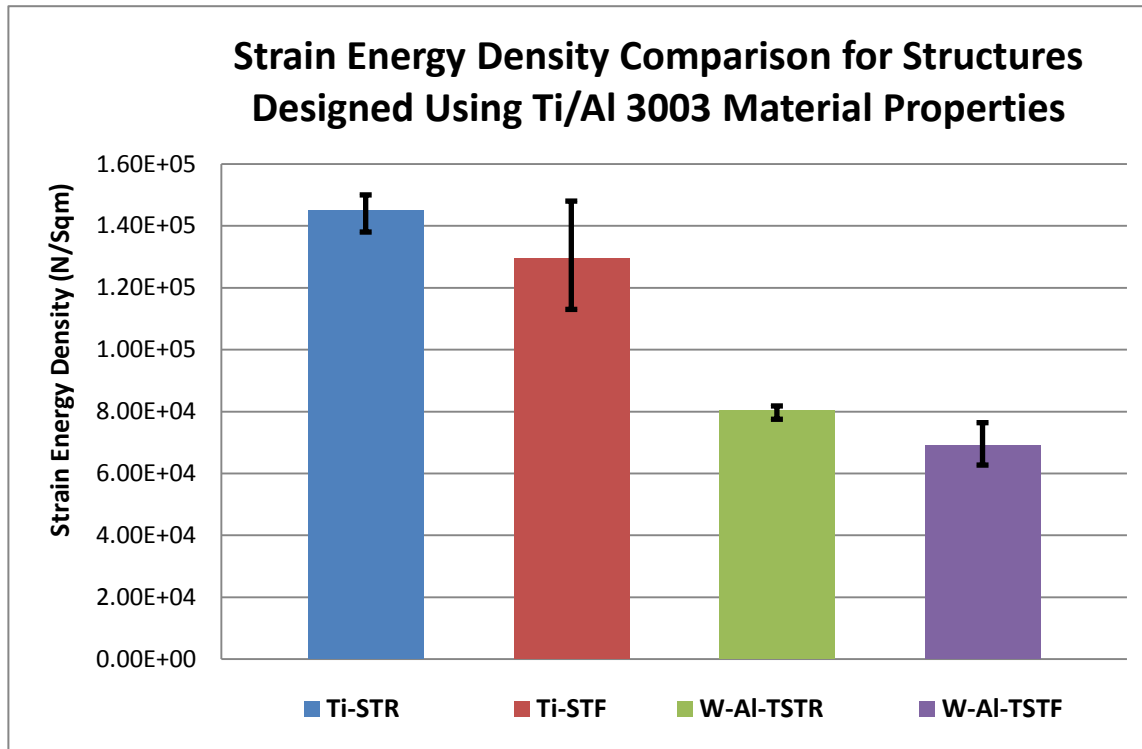


**Figure 7: Strain energy densities for structures designed based on Ti/Al 3003 material properties**

### 3.3 Statistical Analysis of the Strain Energy Density

The results of the strain energy densities presented above were analyzed statistically using SAS 9.1 to verify whether or not their differences are significant. The experiment was a two way factorial design with three replicates. The analyses combine the results of the MetPreg<sup>®</sup>/Al3003 and Ti/Al3003 based structures all in one. Structure design criteria and material used were the two fixed factors used for the analyses. For the purpose of this statistical analysis, alphabetical letters were assigned to groups of experimental units based on the material used as follows: A = Met-STR and Met-STF; B = Ti-STR and Ti-STF; C = Al-STR and Al-STF; D = W-Al-MSTR and W-Al-MSTF; and E = W-Al-TSTR and W-Al-TSTF. Thus, material as a factor comprise five levels while the design as a factor comprise two levels 1 and 2

corresponding to structures designed based on maximum strength and maximum stiffness respectively.

The result of the analysis shows that the data satisfies the assumption of approximate normality and homoscedasticity. Analysis of variance (ANOVA) in Table 10 shows that the two factors and their interactions have significant effects on the response variable. Using factor-level comparison in the least square means (LSMEANS) table (that is, Table 11 below) and the interaction plots in Fig. 8, it is evident that the difference of means between Met-STR and Met-STF is statistically significant. Met-STR and Ti-STF also have significantly different means. However, the difference between the means of Met-STR and Ti-STR is marginally insignificant. Between Ti-STR and Ti-STF as well as between Met-STF and Ti-STF there is no significant difference of mean strain energy density.

Comparing each of the reinforced structures with the un-reinforced ones, Met-STF and W-Al-MSTR have statistically insignificant different means, although the former yielded higher average strain energy density. Also, Ti-STF and W-Al-MSTR have statistically insignificant different means, although the former yielded higher average strain energy density. Apart from these two cases, all reinforced structures have significantly different mean strain energy densities when compared with the single material structures. Post hoc means analysis data in Table 12 for the individual factors shows that structures designed based upon maximum strength criterion have significantly higher average strain energy density than those designed based upon maximum stiffness criterion. Also, all the material categories have statistically significant different average strain energy densities with MetPreg<sup>®</sup> reinforced materials yielding the highest value.

From this analysis, it can be inferred that UC fabricated structures with appropriate reinforcement leads to significant improvement of their load carrying capability compared to fabrications with the matrix materials only. Although MetPreg<sup>®</sup> reinforced structures performed better than titanium reinforced ones with corresponding design criteria, Ti can be considered as a good reinforcement material. This is because the Ti volume fraction of 25% was considerably lower than the 60% volume fraction of MetPreg<sup>®</sup> in the same matrix material. The higher cost of MetPreg<sup>®</sup> makes titanium a good alternative, although the former has higher specific strength than the latter.

**Table 10: Analysis of Variance of the Experimental Data**

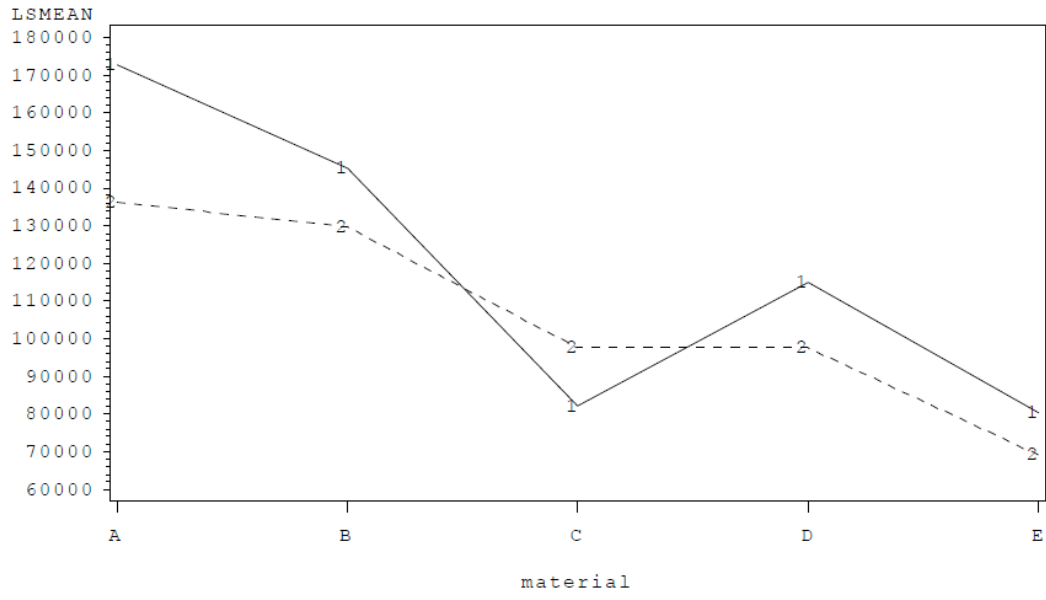
<b>Source</b>	<b>DF</b>	<b>Type III SS</b>	<b>Mean Square</b>	<b>F Value</b>	<b>Pr &gt; F</b>
<b>material</b>	4	26200922369	6550230592	65.92	<.0001
<b>design</b>	1	1272562044	1272562044	12.81	0.0019
<b>material*design</b>	4	2084771809	521192952	5.25	0.0047

**Table 11: Tukey's LSMEAN Adjustment for Multiple Comparison**

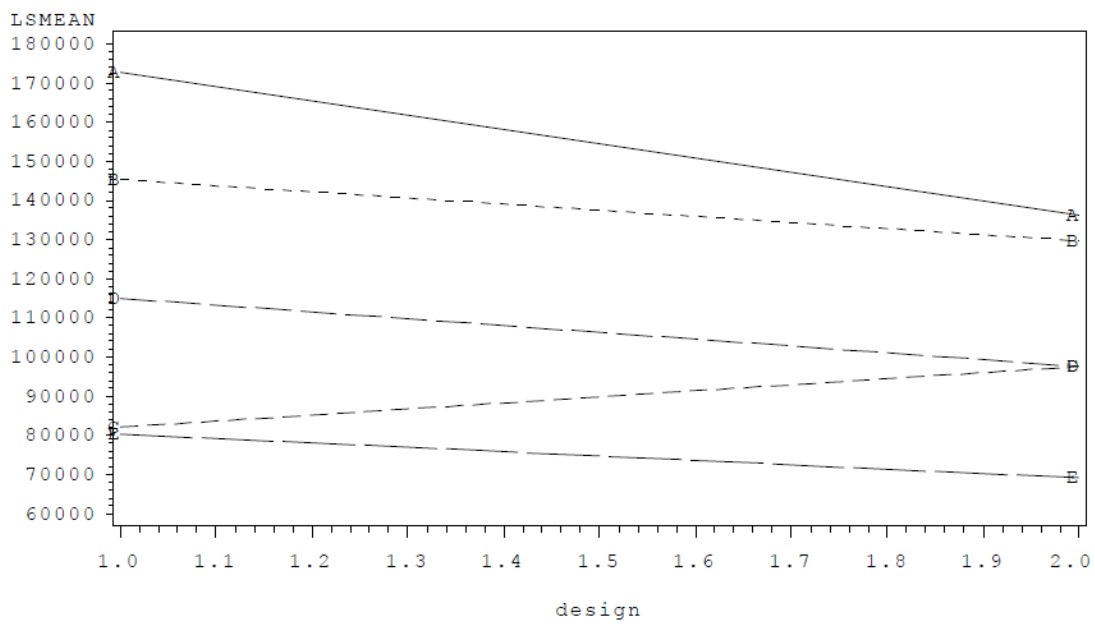
material	design	sed LSMEAN	LSMEAN Number
A	1	172666.667	1
A	2	136266.667	2
B	1	145333.333	3
B	2	129666.667	4
C	1	82063.000	5
C	2	97566.667	6
D	1	115000.000	7
D	2	97600.000	8
E	1	80300.000	9
E	2	69133.333	10

Least Squares Means for effect material*design Pr >  t  for H0: LSMean(i)=LSMean(j)										
Dependent Variable: sed										
i/j	1	2	3	4	5	6	7	8	9	10
1		0.0069	0.0720	0.0012	<.0001	<.0001	<.0001	<.0001	<.0001	<.0001
2	0.0069		0.9773	0.9975	<.0001	0.0037	0.2735	0.0038	<.0001	<.0001
3	0.0720	0.9773		0.6542	<.0001	0.0003	0.0341	0.0003	<.0001	<.0001
4	0.0012	0.9975	0.6542		0.0003	0.0216	0.7270	0.0218	0.0002	<.0001
5	<.0001	<.0001	<.0001	0.0003		0.6663	0.0174	0.6639	1.0000	0.8387
6	<.0001	0.0037	0.0003	0.0216	0.6663		0.5218	1.0000	0.5341	0.0550
7	<.0001	0.2735	0.0341	0.7270	0.0174	0.5218		0.5242	0.0109	0.0005
8	<.0001	0.0038	0.0003	0.0218	0.6639	1.0000	0.5242		0.5317	0.0546
9	<.0001	<.0001	<.0001	0.0002	1.0000	0.5341	0.0109	0.5317		0.9223
10	<.0001	<.0001	<.0001	<.0001	0.8387	0.0550	0.0005	0.0546	0.9223	





(a)



(b)

**Figure 8: Interaction plots between the factors**

**Table 12: Post Hoc Means Analysis for the Individual Factors**

**12a : Design**

<b>Means with the same letter are not significantly different.</b>			
<b>REGWQ Grouping</b>	<b>Mean</b>	<b>N</b>	<b>design</b>
A	119073	15	1
B	106047	15	2

**12b: Material**

<b>Means with the same letter are not significantly different.</b>			
<b>REGWQ Grouping</b>	<b>Mean</b>	<b>N</b>	<b>material</b>
A	154467	6	A
B	137500	6	B
C	106300	6	D
D	89815	6	C
E	74717	6	E

### 3.4 Failure Features

The failure features of the structures depend mostly on the design criterion used. Most of those designed based on maximum stiffness criterion failed at the flange as shown in Fig. 9 for any material combination. Their flange widths are generally smaller than those designed based on maximum strength criterion. It shows that higher stresses are concentrated at the neck of the flanges. Rather than fracture by tearing the materials, most of them deform and in some cases, the consolidated foils delaminate as shown Fig. 10. However, none of the maximum strength structures failed at the flange. MetPreg<sup>®</sup> reinforced maximum strength structures generally failed at the left hand side tension members. The failures occurred on those members at the edge-to-edge foil joints of the Al 3003 matrix materials or at the edge-to-edge joint of the reinforcing MetPreg<sup>®</sup> materials. The right hand side tension members did not have any foil joint; as such no fracture occurred on them. The left tension members were cut perpendicular to the direction of consolidated foils, this make them to have intra-layer edge-to-edge joints. The right hand tension members were however, cut along the direction of foil consolidation. The properties of the joints have been characterized in earlier work (Obielodan et al., 2010A)



**Figure 9: Failure feature of a structure designed based on maximum stiffness criterion**



**Figure 10: Delamination at the flange for some of the structures designed based on the maximum stiffness criterion**

Figures 11 to 13 illustrate the modes of failure for the MetPreg<sup>®</sup>/Al3003 reinforced materials. In Fig. 11, failure occurred at the foil edge-to-edge joints of the matrix material. The stress on the tension member for this structure at failure was 313MPa. A defective matrix material foil joint must have exposed the reinforcing MetPreg<sup>®</sup> foil to cause failure. Figure 12 shows a combination of failures at the matrix foil joints and the joints of the reinforcing materials. There were inter-lamina foil delaminations between the fracture locations. The stress on the tension member at the point of fracture was 320MPa. In Fig. 13, failure occurred at the edge-to-edge joint of the reinforcing MetPreg<sup>®</sup> foils only. The tension member failed at 309MPa.

It is worthy of note that most ultrasonically consolidated MetPreg<sup>®</sup>/Al3003 composite (of the same MetPreg<sup>®</sup> volume fraction, that is 60%) tensile specimens preliminarily tested before these structures were fabricated failed prematurely at stresses ranging from 300 to 450MPa. The Al<sub>2</sub>O<sub>3</sub> reinforcing fibers in the MetPreg<sup>®</sup> foils may have been damaged under the action of the ultrasonic energy applied through the sonotrode during welding, resulting in premature brittle failures of the MetPreg<sup>®</sup>/Al3003 composite members. For the structures designed based on maximum strength criteria using the MetPreg<sup>®</sup>/Al3003 material combination, the stresses on the tension members with foil edge-to-edge joints generally determined the failure point.



**Figure 11: Fracture at the edge-to-edge foil joint of the matrix material on a MetPreg<sup>®</sup> reinforced tension member.**



**Figure 12: Fracture at both the edge-to-edge foil joint of the matrix material and the edge-to-edge joint of the reinforcing foils on a MetPreg<sup>®</sup> reinforced tension member.**

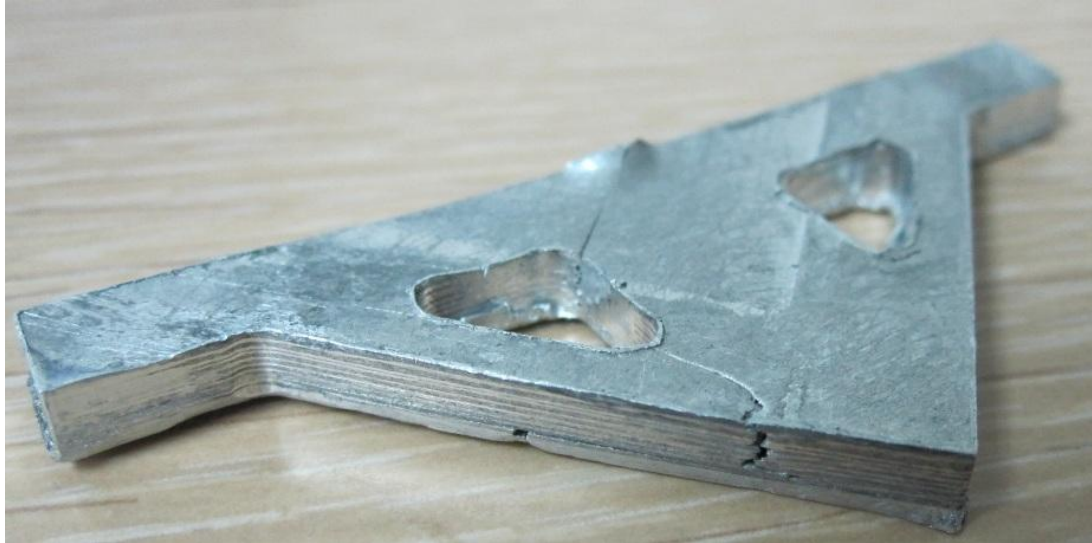


**Figure 13: Fracture at the edge-to-edge joint of the reinforcing foils on a MetPreg<sup>®</sup> reinforced tension member.**

Details of the failure stresses on the tension members of structures designed with MetPreg<sup>®</sup>/Al3003 using maximum strength criterion and their single material copies are shown in Fig. 14 (that is, those described with STR labels). Al-STR structures ultrasonically consolidated exclusively with Al3003 foils and default foil overlap setting of width 23.90mm fractured at the tension member at an average stress of 169MPa. This fracture stress is within the range of tensile strengths obtained for tensile specimens fabricated with the same machine parameters in earlier work (Obielodan *et al.*, 2010A). Also, the W-Al-MSTR structures fabricated exclusively with the wrought Al3003 substrate material failed at the tension member at an average stress of 205MPa, which is within the range of the tensile strengths obtained for the parent material.

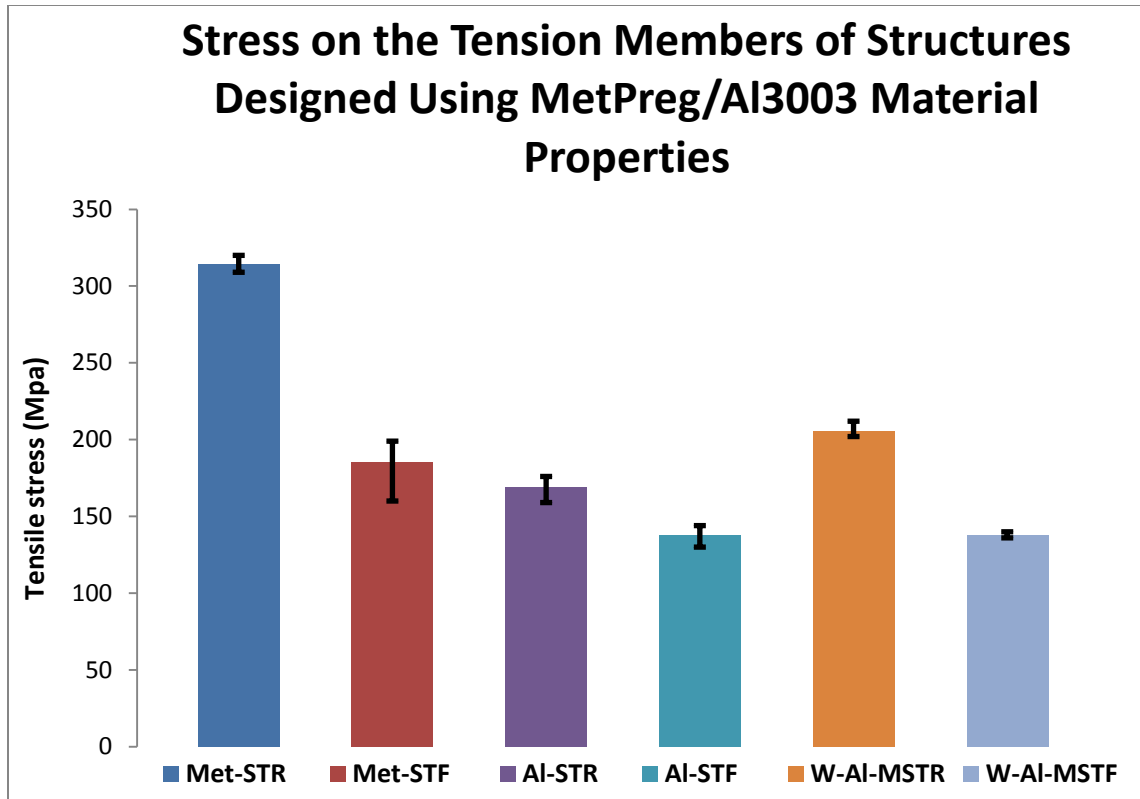


**Figure 14: Stress on the tension members of structures designed using MetPreg<sup>®</sup>/Al 3003 material properties at the point of failure**

#### 4 Conclusions

The use of the ultrasonic consolidation process for the fabrication of multi-material minimum weight structure has been demonstrated. A fabrication methodology for joining foils of different materials to make dual-material structures was developed. Test results show that there are significantly higher strain energy densities at the point of failure in structures with reinforced members compared to those fabricated with Al 3003 matrix materials only. As a result, their load carrying capacities were greatly improved. It was observed that the failure mode of the structures is generally dependent upon the design criteria and the materials used. Structures fabricated based upon maximum strength criterion using MetPreg<sup>®</sup>/Al3003 composite materials as the tension members exhibited brittle failures at edge-to-edge foil joints. Those designed based upon



maximum stiffness criterion generally failed at the flange of the triangular structure irrespective of the material combination. From the results of this work, it is believed that multi-material structures can be fabricated for real life applications using appropriate material combinations.

## References

- Arcaute K., Mann B, and Wicker R. 2009. Stereolithography of spatially controlled multi-material bioactive poly(ethylene glycol) scaffolds, *Acta biomaterialia*, 6(3), pp.1047-1054
- Cohen D.L., Malone E., Lipson H. Bonassar L.J., 2006. “Direct Freeform Fabrication of Seeded Hydrogels in Arbitrary Geometries”, *Tissue Engineering*, 12(5), pp.1325-1335.
- Dewhurst Peter, 2001. Analytical solutions and numerical procedures for minimum-weight Michell structures, *Journal of the Mechanics and Physics of Solids*, 49(3) 445 – 467
- Dewhurst Peter, 2005. A general optimality criterion for strength and stiffness of dual-Material property structures, *International journal of mechanical sciences*, 47(2), pp.293-302.
- Domack M.S., and Baughman J.M., 2005. Development of nickel-titanium graded composition components, *Rapid prototyping journal*, 11(1), pp.41-51.
- Foroozmehr E., Sarrafi R., Hamid S. and Kovacevic R. Synthesizing of functionally graded surface composites by laser powder deposition process for slurry erosion applications. *Proceedings of 20<sup>th</sup> solid freeform fabrication symposium*, Austin, TX, USA, August 3-5, 2009.
- Griffith M.L., Harwell L.D., Romero J.T., Schlienger E., Atwood C.L., Smugeresky J.E.,. Multi-material processing by LENS, *Proceedings of the 8<sup>th</sup> solid freeform fabrication symposium*, Austin, TX, PP.387, 1997
- Inamdar A., Magana M., Medina F., Grageda., Wicker R. “Development of automated multiple material stereolithography machine”, *Proceedings of the 17<sup>th</sup> solid freeform fabrication symposium*, Austin, TX, USA, August 2006.
- Jae-Won Choi J., MacDonald E., and Wicker R. Multiple material microstereolithography. *Proceedings of 20<sup>th</sup> solid freeform fabrication symposium*, Austin, TX, USA, August 3-5, 2009

- Janaki Ram G.D. and Brent Stucker, 2008. LENS<sup>®</sup> deposition of CoCrMo coatings on titanium implant structures, *Journal of manufacturing science and engineering – Transactions of the ASME*, 130(2), pp. 024503-1 to 024503-5.
- Janaki Ram G.D., Robinson C., Yang and Stucker B.E., 2007. Use of ultrasonic Consolidation for multi-material structures”, *Rapid prototyping journal*, 13(4), pp.226-235.
- Kruger S., Wagner G. and Eifler D., 2004. Ultrasonic welding of metal/composite joints, *Advanced engineering materials*, 6(3), pp.157-159.
- Liu W., and DuPont J.N., 2003. Fabrication of functionally graded TiC/Ti composites by laser engineered net shaping, *Scripta materialia*, 48(8), pp.1337-1342
- Malone E., Rasa K., Cohen D., Isaacson T., Lashley H., Lipson H., 2004. “Freeform Fabrication of Zinc-Air Batteries and Electromechanical Assemblies”, *Rapid Prototyping Journal*, 10(1), pp.58-69.
- Michell, A.G.M., 1904, Limits of economy of material in frame-structures, *Philosophical magazine*, 8(47), pp.589-597.
- Obielodan J.O. and Stucker B.E. Effects of post processing heat treatments on the bond quality and mechanical strength of Ti/Al3003 dual materials fabricated using ultrasonic consolidation, *Proceedings of the 20<sup>th</sup> solid freeform fabrication symposium*, Austin, TX, USA, August 3-5, 2009.
- Obielodan J.O., Janaki Ram G.D., Stucker B.E., Taggart D.G., 2010A. Minimizing defects between adjacent foils in ultrasonically consolidated parts, *Journal of engineering materials and technology*, 132(1), pp. 011006-1 - 011006-8
- Obielodan J.O., Ceylan A., Murr L.E., Stucker B.E., 2010B. Multi-material bonding in ultrasonic consolidation, *Rapid prototyping journal*, 16(3), pp.180-188
- Selyugin S.V., 2004. Some general results for optimal structures, *Structural and Multi-disciplinary optimization*, 26(5), pp.357-366.
- White D.R., 2003. Ultrasonic consolidation of aluminum tooling, *Advanced materials & processes*, 161(1), pp.64-65.
- Wicker R. Medina F. and Elkins C. Multiple material micro-fabrication: extending stereolithography to tissue engineering and other novel applications, *Proceedings of solid freeform fabrication symposium*, Austin, TX, USA, August 2004.